Photodetector with integrated optical thin film filters

Photodetector with integrated optical thin film filters

M A Vieira[1,3,4], **M Vieira**[1,2], **P Louro**[1,2], **V Silva**, **A S Garção**[2,3]
[1]Electronics Telecommunication and Computer Dept. ISEL, Lisboa, Portugal.
[2]CTS-UNINOVA, Quinta da Torre, Monte da Caparica, 2829-516, Caparica, Portugal.
[3]DEE-FCT-UNL, Quinta da Torre, Monte da Caparica, 2829-516, Caparica, Portugal.

E-mail: mv@isel.ipl.pt

Abstract. This paper reports on optical filters based on a-SiC:H tandem pi´n/pin heterostructures. The spectral sensitivity is analyzed. Steady state optical bias with different wavelengths are applied from each front and back sides and the photocurrent is measured. Results show that it is possible to control the sensitivity of the device and to tune a specific wavelength range by combining radiations with complementary light penetration depths. The transfer characteristics effects due to changes in the front and back optical bias wavelength are discussed. Depending on the wavelength of the external background and irradiation side, the device acts either as a short-or a long-pass band filter or as a band-stop filter. The output waveform presents a nonlinear amplitude-dependent response to the wavelengths of the input channels.

1. Introduction

Optical communication in the visible spectrum usually interfaces with an optoelectric device for further signal processing. There has been much research on semiconductor devices as elements for optical communication [4,5,6]. Multilayered Si/C structures based on amorphous silicon technology are expected to become reconfigurable to perform WDM optoelectronic logic functions. Filters are used to emphasize signals in a certain wavelength range and to reject signals in other ranges. They have a nonlinear magnitude-dependent response to each incident light wave. This nonlinearity provides the possibility for selectively removing and adding wavelength and can be used to boost signal after multiplexing or before demultiplexing.

An optoelectronic device converts light photons to electrons that mimic the light signal in such way that data transmitted by the light beam can be received and processed further with electrical circuits. These devices have one surface over which the optical signal shines. On our device, a multilayered Si/C heterostructure light [7, 8] can shine on the two surfaces namely back and front. This device acts as an optical filter when other fixed wavelengths superimpose the incident light data signal on the surface it shines with. By selecting a wavelength on either the red or blue part of the spectrum the device can be tuned as a filter and used as a wavelength division multiplexing-demultiplexing technique, WDM [9]. This device has been characterized with a model with its experimental verification. Here, we propose a photodetector with integrated optical thin film filters. By means of optical control signals applied to the device, the photonic function may be

[4] To whom any correspondence should be addressed.

modified giving reconfiguration. A new method is presented for optical routing using wavelength background processing techniques.

2. Device optimization and characterization

The sensor element is a multilayered heterostructure based on Si:H and a-SiC:H. The configuration shown in figure 1 includes two stacked p-i-n structures sandwiched between two transparent contacts. The thicknesses and optical gap of the front í'-(200nm; 2.1 eV) and back i-(1000nm; 1.8eV) layers are optimized for light absorption in the blue and red ranges, respectively. Spectral response measurements without and under different optical bias and frequencies were performed in order to test the devices sensitivity.

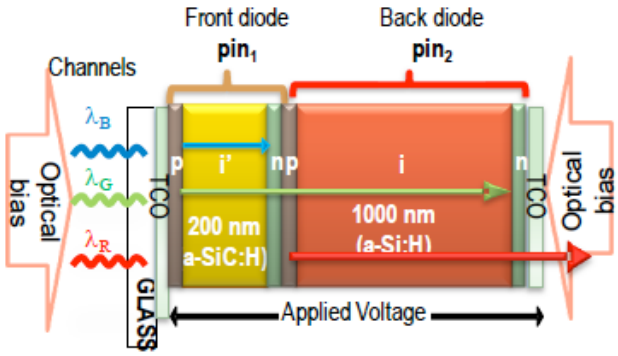

Figure 1. Device configuration and operation

The device operates within the visible range using as input color channels (data) the wave square modulated light (external regulation of frequency and intensity) supplied by a red (624 nm; 51 μW/cm^2), a green (526 nm; 73 μW/cm^2) and a blue (470 nm; 115 μW/cm^2) LED. Additionally, steady state violet (400 nm, 2800 μW/cm^2), red (624 nm, 652 μW/cm^2), green (524 nm, 580 μW/cm^2) and blue (470 nm, 680 μW/cm^2) illumination (optical bias) was superimposed from the front (pin1) and back (pin2) sides in LEDs driven at different current values. The spectral sensitivity was analyzed by applying different wavelength optical bias from the front and backsides of the device (see figure1). Under front irradiation, the spectral photocurrent without light bias control at -8V applied voltage and different frequencies (250 Hz-3500Hz) is shown in figure 2.

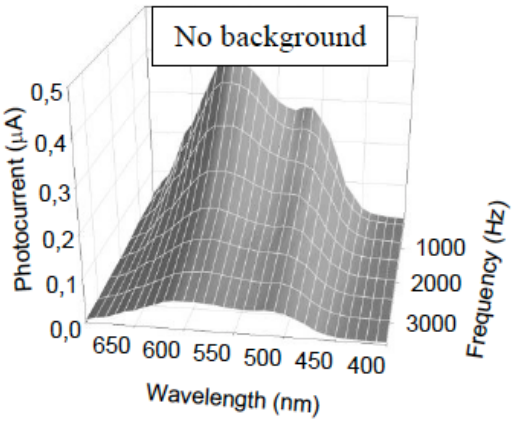

Figure 2. Spectral photocurrent without light bias control from the front side.

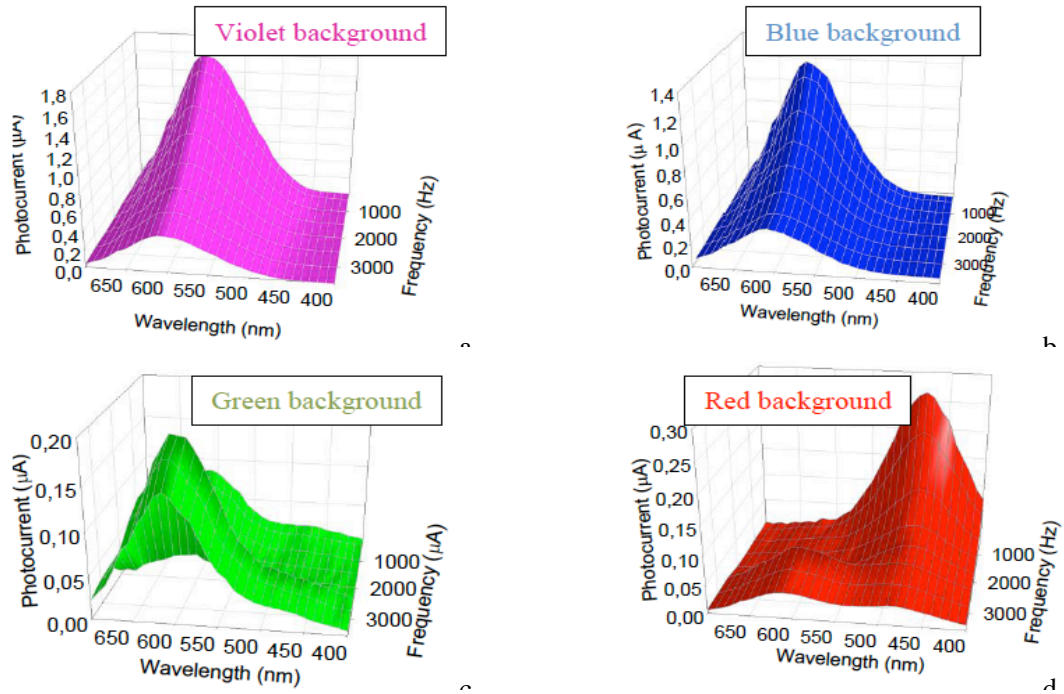

Figure 3. Spectral photocurrent under violet (a) blue (b) green (c) and red (d) bias control applied from the front side.

Under front irradiation, in figure 3 it is displayed the spectral photocurrent for different frequencies under violet (a), blue (b), green (c) and red (d) light bias control at -8V applied voltage and different frequencies (250 Hz-3500Hz). Results show that the spectral response depends strongly on the bias control wavelength and frequency. As the bias control wavelength increases the spectral sensitivity shifts to the low wavelength spectral regions and decreases with the frequency, suggesting capacitive effect across the device.

In figure 4 it is displayed the spectral photocurrent at 3500 Hz, under red, green, blue and violet background irradiations (colour symbols) and without it (black symbols) applied from the front (a) and back (b) diodes. For comparison the spectral photocurrent (right axis) for the front, p-i'-n and the back, p-i-n, photodiodes (dash lines) are superimposed.

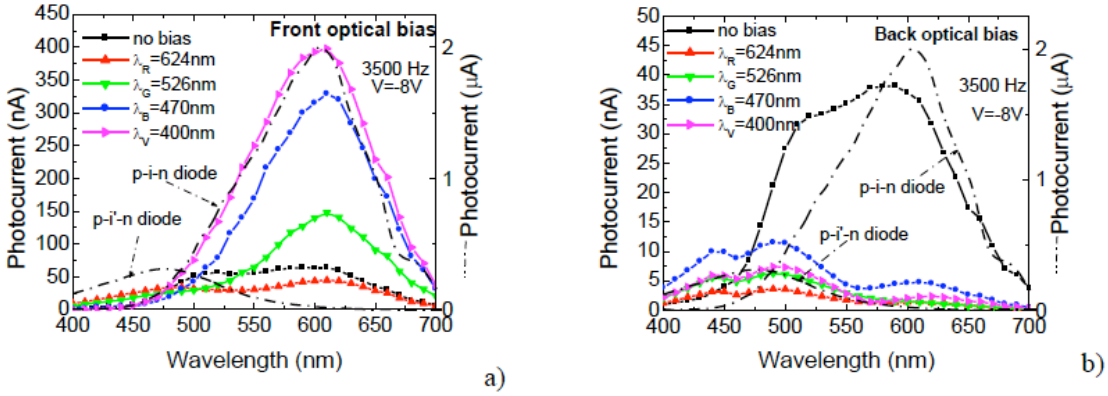

Figure 4. Spectral photocurrent under red, green, blue and violet background irradiations (color symbols) and without it (black symbols) applied from the front (a) and back (b) diodes.

Results show that the spectral sensitivity under steady state irradiation depends on its wavelength and on the impinging side. Under front irradiation, the back diode photoresponse is tuned and the sensitivity strongly increases for wavelengths higher than 500 nm when compared with its value without optical bias. As the background wavelength decreases, the spectral response increases. Under back irradiation the front diode photoresponse is selected. The sensitivity strongly increases in the short wavelengths range and collapses in the long wavelength region.

3. Transfer characteristics

In figure 5, at 3500 Hz, it is displayed the ratio between the photocurrent under different optical bias and without it (gain) under front (symbols) and back (lines) irradiations: red (α^R), green (α^G), blue (α^B) and violet (α^V).

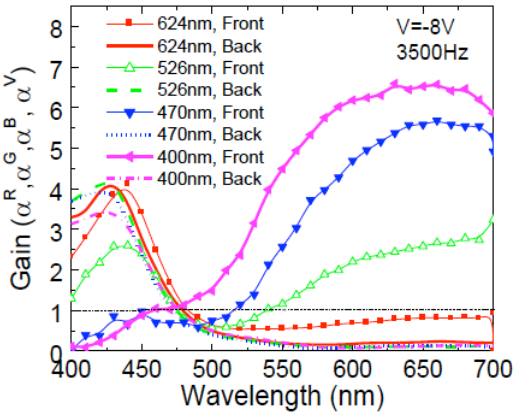

Figure 5. Gain under front (symbols) and back (lines) irradiations: red (α^R), green(α^G), blue (α^B), violet (α^V).

Under back irradiation (lines) the gain does not depend on the wavelength of the background. The spectral sensitivity in the low wavelength range is enhanced and the device always acts as a short-pass filter. Under front irradiation (symbols) the filter properties of the device depend on the background wavelength. Under red irradiation (figure 3d) the gain is high in the short wavelengths range acting the device as a short-pass filter. Under violet (figure 3a) and blue (figure 3b) irradiations, the transfer function presents an enhanced gain in the long wavelength range acting as a long-pass filter. Under front green background, the device (figure 3c) is a band-rejection active filter for frequencies higher than 2000Hz that works to screen out wavelengths that are within the medium range (475nm-550nm) giving easy passage at all wavelengths below and above.

Results confirm that under controlled wavelength backgrounds it is possible to fine-tune the spectral sensitivity of the device. Its sensitivity is strongly enhanced ($\alpha>1$) in a specific wavelength range and quenched ($\alpha<1$) in the others, tuning or suppressing a specific band. The sensor is a wavelength current-controlled device [10] that makes use of changes in the wavelength and impinging side of the optical bias to control the power delivered to the load. Self-optical bias amplification or quenching under uniform irradiation is achieved. By using background lights with complementary light penetration depths across the pi´n/pin device and changing the irradiation side, it is possible to control the spectral response and to filter a specific wavelength band.

4. Photonic active filters

To analyze the device under information-modulated wave and uniform irradiation, three monochromatic pulsed lights separately (red, green and blue input channels) or their combination (MUX signal) illuminated the device. Steady state red (652μ Wcm^{-2}), blue (680μ Wcm^{-2}) and violet (2800μ Wcm^{-2}), optical bias was superimposed separately from the front (pin1) and the back

(pin2) sides and the photocurrent measured at -8 V. In Table 1 the gains (α) of the individual channels, defined as the ratio between photocurrents under irradiation (ON state) and without it (OFF state), for the red, green, and blue input channels are presented. Here, the superscripts are related to the background wavelength (R, G, B, V) and the subscripts (Rpin1,2,G pin1,2 B pin1,2) to the channel color and irradiation side.

Table 1. Gains (αR,G.B,pin1,2) at the input red, green, and blue channels wavelengths

Channels	α^R	α^G	α^B	α^V
$\alpha_{R,pin1}$	0,62	1,28	3,00	5,13
$\alpha_{R,pin2}$	0,12	0,42	0,47	0,34
$\alpha_{G,pin1}$	0,63	0,85	1,52	2,40
$\alpha_{G,pin2}$	0,59	0,62	0,67	0,67
$\alpha_{B,pin1}$	1,39	1,00	0,81	1,11
$\alpha_{B,pin2}$	2,22	1,94	1,97	1,64
$\alpha_{V,pin1}$	11,57	5,80	1,60	1,00
$\alpha_{V,pin2}$	11,57	13,90	1,20	10,42

Results show that, even under transient conditions, the effect of the background wavelength and impinging side presents the same nonlinear dependence as in figure 5. The morphology of the filter results from the interaction of the electric field under applied optical bias (red, green, blue, violet) and the transient electric field induced by the input channels (red, green, blue and violet). Under back irradiation, the small absorption depth of the violet photons across the back diode quenches the electric field there and as a consequence the red collection (Red ON) almost disappears (α^VR,pin2<<1). The blue channel is absorbed across the front diode where the electric field was enhanced resulting in an increase collection of the channel (α^V B,pin2>1). Since the green channel is absorbed across front and back diodes, its collection is balanced by the increase collection in the front diode and its reduction at the back (α^VG,pin2~1). The front violet background is absorbed at the surface of the front diode, increasing the electric field at the back diode, where the red and part of the green channels generate optical carriers. So, the collection is strongly enhanced (α^VR,pin1>>1, α^VG,pin1>1) while the blue collection stays near its dark value (α^VB,pin1~1).

The polychromatic combinations of the same red, green, blue and violet input channels with gains presented in Table 1 was used to generate a multiplexed (MUX) signal.

In figure 6, the filtered signals under front (pin1) and back (pin2) violet light control are displayed. The signals were normalized to the maximum intensity under violet front irradiations to suppress the dependence on sensor and LEDs positioning. The bit sequences used to transmit the information are shown at the top of the figures.

Different gains for the RGB channels were obtained (Table 1). Due to this wavelength non-linearity under front violet background, the encoded multiplexed signal presents as many levels as the possible RGB combinations, in a maximum of 2^3(eight-level encode). Those levels can be grouped into two main classes due to the high amplification of the red channel (α^VR,pin1>>1). The upper levels are ascribed to the presence of the red channel and the lower to its absence allowing the red channel decoder. Since under front irradiation the green channel is amplified (α^VG,pin1>1), the highest levels, in both classes, are ascribed to the presence of the green channel and the lower ones to its lack (long-pass filter). Under back irradiation the red channel is suppressed (α^VR,pin2<<1), the blue enhanced (α^VB,pin2>1) and the green reduced(α^VG,pin2<1), so the

encoded multiplexed signal presents a maximum of four separate levels (2^2). The highest levels correspond to the presence of the blue channel ON with or without the green ON respectively, and the other to its absence. The blue channel is then decoded using this simple algorithm (short-pass filter).

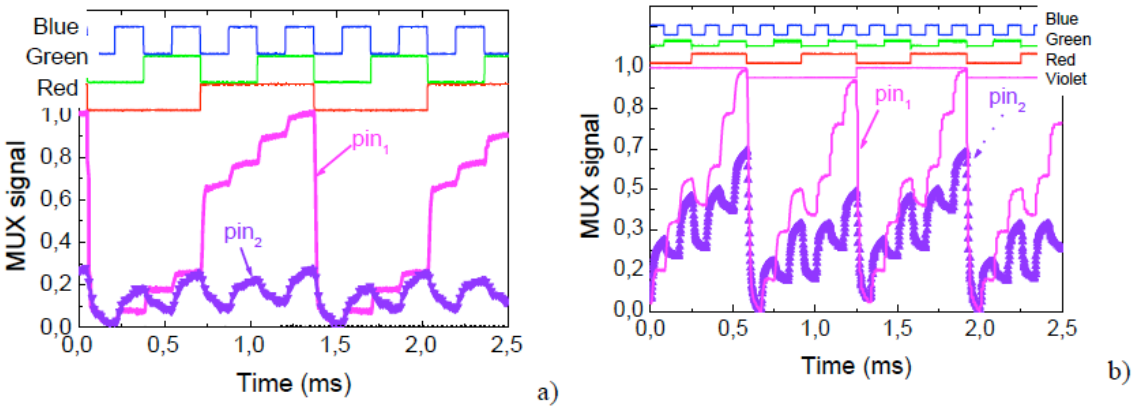

Figure 6. Filtered output signals under front (pin1; lines) and back (pin2; symbols) violet irradiation. a) Red, Green and Blue channels. b) Red, Green, Blue and Violet channels. On the top of the figures the optical signals used to transmit the information guide the eyes.

To test the algorithm, a polychromatic combination of the same red, green and blue input channels of figure 6a, in a different bit sequence, was used to generate a multiplexed (MUX) signal. In figure 7 the filtered signals under front (pin1) and back (pin2) violet light control are displayed. The signals were normalized to the maximum intensity under violet front irradiations to suppress the dependence on sensor and LEDs positioning. The decoded signal is shown on the top of the figure showing the effectiveness of the simple algorithm. Results show, that by means of violet optical bias control, the MUX photonic function may be modified giving reconfiguration. This new method based on wavelength background processing techniques enables the optical routing.

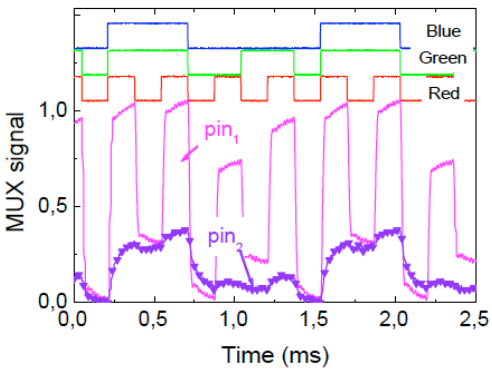

Figure 7. Filtered output signals: front (pin1; lines) and back (pin2; symbols) violet irradiation. On the top, the decoded signal is displayed.

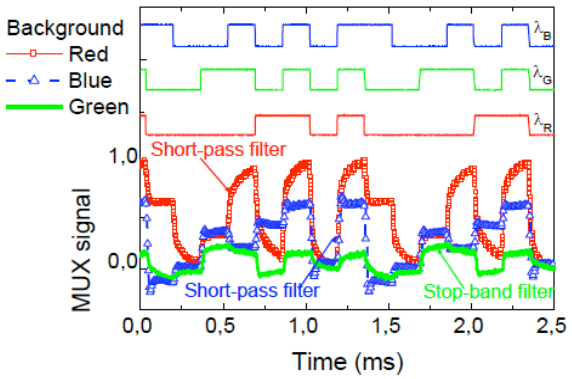

Figure 8. Filtered output signals under front red, green and blue background. The bit sequences used to transmit the information are shown at the top of the figures.

5. Optical bias controlled filtering

In figure 8, the filtered signals under red and green blue light control are displayed with the colour lines ascribed to the front background wavelength. The signals were normalized to the maximum intensity under red front irradiations. The bit sequences used to transmit the information are shown at the top of the figure.

Taking into account table 1, under red background, the red channel response is reduced ($\alpha^R R<1$) and the blue ($\alpha^R B>1$) and green ($\alpha^R G>1$) ones increased. The red channel is rejected (short-pass filter), so the mixture of both blue and green is recovered. The filtered signal is a 4-level encoding (2^2). Under blue irradiation, the optical bias effect is opposite and the blue channel is rejected (long-pass filter). So, the change in the transmitted information is due exclusively to the presence of both red and green channels. The filtered signal becomes a 4-level encoding (22^2). Under green irradiation, the devices act as a stop-band filter that drops the green channel. By subtracting the output signal under irradiation from the signal without it, the green channel is decoded. Here, the filtered information is mainly a 2^1 level encoded data.

6. Conclusions

Integrated photonic filters based on SiC multilayer devices were analyzed and their transfer functions presented, showing that the light-activated pi'n/pin a-SiC:H devices combine the demultiplexing operation with the simultaneous photodetection and self-amplification of an optical signal. Reconfiguration was provided by background wavelength control. Results show that the background wavelength and irradiation side control the output signal. By using background lights with complementary light penetration depths and changing the irradiation side, it is possible to change the spectral response and to filter a specific wavelength band acting either as a short- or a long- pass band filter or as a band-stop filter.

Acknowledgements

This work was supported by PTDC/EEA-ELC/111854/2009, PTDC/EEA-ELC/115577/2009 and PTDC/EEA-ELC/120539/2010.

7. References

[1] Connelly M J 2002 *Semiconductor Optical Amplifiers (*Boston, MA: Springer-Verlag) ISBN 978-0-7923-7657-6

[2] Petit C and Blaser M 2006 Photodiodes with integrated optical filters for passive optical network applications *Workshop on Optical Components for Broadband Communication* (ed. by Pierre-Yves Fonjallaz, Thomas P. Pearsall) Proc. of SPIE Vol. 6350 63500I

[3] Ibrahim S, Luo L W, Djordjevic S S, Poitras C B, Zhou I, Fontaine N K, Guan B, Ding Z, Okamoto K, Lipson M and Yoo S J B 2010 Fully reconfigurable silicon photonic lattice filters with four cascaded unit cells paper OWJ5. *Optical Fiber Communications Conference* OSA/OFC/NFOEC (San Diego, 21 Mar 2010)

[4] Vieira M, Louro P, Fernandes M, Vieira M A, Fantoni A and Costa J 2011, "Three Transducers Embedded into One Single SiC Photodetector: LSP Direct Image Sensor, Optical Amplifier and Demux Device",*Advances in Photodiodes*, Gian Franco Dalla Betta (Ed.), ISBN: 978-953-307-163-3 (InTech Chap 19) pp:403-425

[5] Louro P, Vieira M, Vieira M A, Fernandes M and Costa J 2011 Use of a SiC:H Photodiodes in Optical Communications Applications *Advances in Photodiodes*, Gian Franco Dalla Betta (Ed.), ISBN: 978-953-307-163-3 (InTech, Chap 19) pp 377-402)

[6] Igushi Y and Yamabayashi N 2000 Novel rear-illuminated 1.55 μm-photodiode with high wavelength selectivity designed for bi-directional optical transceiver *Proc. 2th Int. Conf. on InP and Related Mater* vol 317 pp 317-320.

[7] Vieira M A, Vieira M, Costa J, Louro P, Fernandes M and Fantoni A 2011 Double Pin Photodiodes with Two Optical Gate Connections for Light Triggering: A Capacitive Two-phototransistor Model *Sensors & Transducers Journal* **10** Special Issue 96-120. ISSN 1726-5479.